SEISMIC RESPONSE OF OFFSHORE WIND MONOPILES IN COHESIONLESS SOILS

J. Seong, University of Cambridge, UK, js2501@cam.ac.uk
C.N. Abadie*, University of Cambridge, UK, cna24@cam.ac.uk
S.K. Haigh, University of Cambridge, UK, skh20@cam.ac.uk
S.P.G. Madabhushi, University of Cambridge, UK, mspg1@cam.ac.uk

ABSTRACT

Development of offshore wind farms in seismic zones requires consideration of monopile foundation design subjected to dynamic earthquake-induced loads. This paper presents the results of a dynamic centrifuge test, investigating the monopile response to seismic loads in dry cohesionless soils. The test involved two identical instrumented monopiles, driven into a layered soil sample, with a loose layer overlying a very dense layer. A servo-hydraulic earthquake actuator was used to generate sine sweep and sinusoidal bedrock motions, during which pile and soil accelerations, dynamic bending moments and pile rotation were assessed. A monotonic push was performed on one of the piles prior to the earthquakes to assess initial capacity, while the second pile was pushed after completion of the dynamic load sequence to establish the post-seismic capacity. The results show strong acceleration amplification for earthquake loading frequencies close to the first mode of frequency of the pile-soil system. The monotonic tests demonstrate that, for the layered sand configuration considered here, the monotonic behaviour of the pile is strongly affected by the dynamic loading history.

Keywords: monopile foundation, seismic loading, centrifuge testing

INTRODUCTION

Offshore wind has developed rapidly over the past decade, mostly in Europe, and has an enormous potential for providing renewable energy across the globe. Methods used for the design of foundations have improved massively over the last 5 to 10 years, enabling significant and robust optimisation of the geometry (e.g. the PISA project - Byrne *et al.*, 2019; Jeanjean *et al.*, 2017; the SOLCYP project - Puech, 2017). However, they focused on quasi-static loading cases, mostly relevant to the North Sea and the Irish Sea. For further development, such as deployment in East Asia and North American waters, a wider range of loading scenarios need to be addressed, and in particular earthquake-induced dynamic loads.

Offshore wind turbines are gigantic structures (e.g. Figure 1), that are commonly supported by monopile foundations. The environmental loads acting on an offshore wind foundation comprise of wind, wave and current-induced hydrodynamic loads, as well as in specific zones, earthquake, snow and ice loads (Figure 1).

Despite the number of projects currently planned and undertaken in seismic zones, the understanding of pile response to earthquake loads is still in its infancy, but is a real concern for designers across the globe (e.g. the ACE project - DNV-GL, 2019). Current guidelines provide limited recommendations on structural design with regards to both earthquakes and earthquake-induced tsunamis (e.g. DNV, 2014, section 4.5.8). For foundation design, the understanding of pile response is limited and current design guidelines recommend to employ the same method as for cyclic design (e.g. see Abadie *et al.*, 2020 for description of the method) and degrade the *p-y* curves using factors that must be evaluated for site-specific conditions (DNV, 2014, section 10.1.4.4). There is no further detail on the range of values for these degradation factors, nor insight on whether the method is applicable or not.

The use of degradation factors to derive the cyclic response was originally proposed by Reese

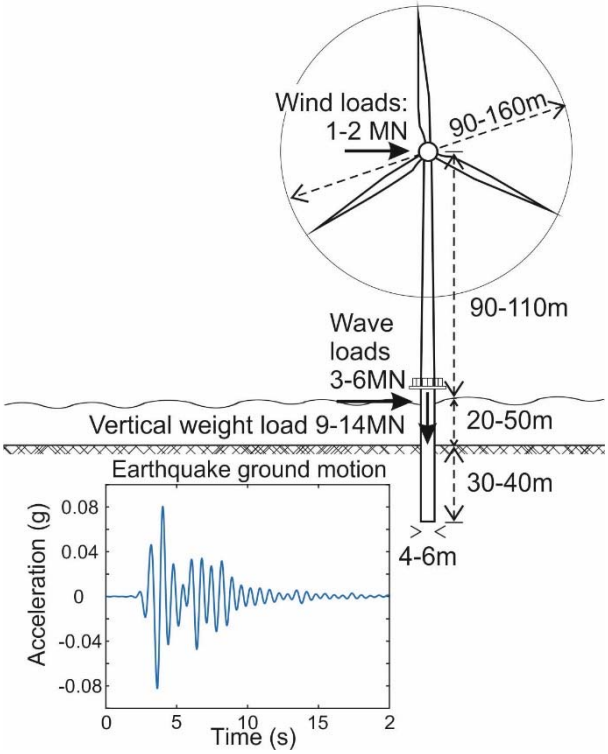

Figure 1. Typical loading and dimensions of offshore wind turbines

et al. (1974), based on field tests performed by Cox *et al.* (1974) for pile geometries and load scenarios adapted to oil and gas pile design. It is broadly acknowledged that these methods are inappropriate for offshore wind piles and significant progress in research worldwide has been published over the last decade to provide improved guidelines for the design of monopiles to cyclic lateral loading (e.g. Abadie, 2015; Abadie *et al.*, 2020; Achmus *et al.*, 2009; Andersen, 2015; Kirkwood, 2015; Klinkvort, 2012; Lau, 2015; LeBlanc *et al.*, 2010a, 2010b; Peralta, 2010; Puech, 2017; Zhang *et al.*, 2016). However, these studies all focus on quasi-static wind and wave-induced cyclic loads and do not address the case of dynamic earthquake-induced loads.

To date, limited research has been performed and published to address this knowledge gap (e.g. Kim *et al.*, 2014). This paper aims to address this issue by providing the first-of-a-kind experimental centrifuge test on large-diameter monopiles subjected to earthquake ground motions, followed by an extreme wind-wave monotonic load on the sub-structure.

EXPERIMENTAL METHODS

This paper examines the result of a dynamic test, undertaken using the 10 m diameter Turner beam centrifuge at the Schofield Centre at the University of Cambridge. The benefits of centrifuge modelling in geotechnics are widely recognised (Madabhushi, 2014), and principally enables to perform reduced-scale model tests while preserving the stress-strain behaviour of the soils by scaling up the gravity by a factor N. Hence, stress and strain similarity is achieved for a soil sample prepared at the same relative density as in the field, and scaling factors originally listed by Schofield (1980) can be used to relate model to prototype behaviours. The test set-up discussed in this paper is shown in Figure 2(a).

Layered soil sample

The tests were conducted using an Equivalent Shear Beam model container (Figure 2(b)), consisting of alternating layers of durnal and rubber rings (Brennan *et al.*, 2006). A layered

Table 1. Properties of Hostun HN31 sand

Property	Symbol	Unit	Value
Minimum void ratio	e_{min}	-	0.555
Maximum dry unit weight	e_{max}	-	1.01
Specific gravity	G_s	-	2.65
Critical angle of friction	ϕ_{crit}	degrees	33
Mean particle size	d_{50}	mm	0.424
Uniformity coefficient	C_u	-	1.67

Table 2. Pile properties

	Embedded length L	Diameter D	Load eccentricity h	Wall thickness t	h/D	h/L	L/D	D/t
Model	200mm	38.1mm	300 mm	1.59 mm	7.87	1.5	5.25	24
Prototype	12 m	2.29 m	18 m	2.86 cm	7.87	1.5	5.25	48

soil profile of Hostun HN31 sand (Table 1) was poured using an automatic sand pourer (Chian *et al.*, 2010) and dry pluviation through air. Two layers were poured: a dense layer at $D_R = 88\%$, overlaid by a loose layer at $D_R = 36\%$. The bottom 50% of the embedded length of the piles was in the dense layer, while the remaining top 50% was in the loose layer, with the rest of the pile above the soil representing the free superstructure of the wind turbine mast, with a lumped mass on the top (Figure 2(a)).

An air hammer was installed at the bottom of the sample, together with accelerometers at selected depth within the soil (Figure 2(a)). This enabled to log the shear wave velocity and determine the small strain shear modulus before and after earthquakes. This is shown in Figure 3, together with profiles obtained following Hardin and Drnevich (1972) and Oztoprak and Bolton (2013).

Piles geometry

The model piles used for testing were the same as those used by Kirkwood (2015) and Lau (2015), for which the dimensions are reminded in Table 2. The test was performed at a centrifugal acceleration of 60g, leading to the prototype pile dimensions listed in Table 2. Due to space restriction, it was not possible to achieve the prototype dimensions of Figure 1; however, the prototype piles are geometrically equivalent to a typical offshore wind monopile, and is representative of a 35 m long monopile scaled down to 1/3. They therefore provide good insight into dynamic monopile behaviour.

Both piles were gently driven in the soil sample using a hammer at 1-g, and hence be considered to be 'wished-in-place'. They were located ~6 diameters apart and ~4.5 diameters from the box walls, enabling sufficient clearance to avoid interaction between the two piles.

Pile-0 (Figure 2) was used as a reference pile and was loaded monotonically prior to triggering any model earthquakes, while Pile-PE was used to assess the effect of seismic loads on monotonic lateral pile capacity. Pile-PE was also instrumented with strain gauges to directly measure the bending moments of the pile. The geometry and location of the strain gauges is shown in Figure 2(a).

In order to simulate the inertia of the blades, turbine, gearbox etc and their effect on the pile response during earthquake ground motion, a lumped mass was located at the top of each pile (Figure 2(c)), representing the combined mass of the upper-structure, nacelle, rotor and blades. The mass was equal to 1.8 kg, corresponding to a vertical load of $V = 4\ MN$.

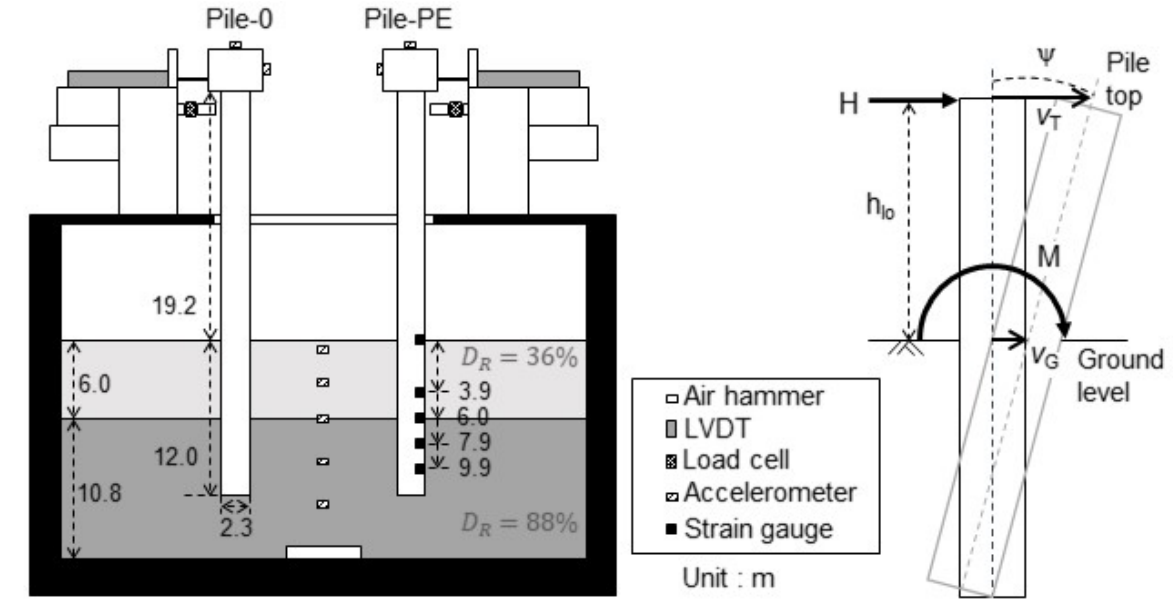

(a)

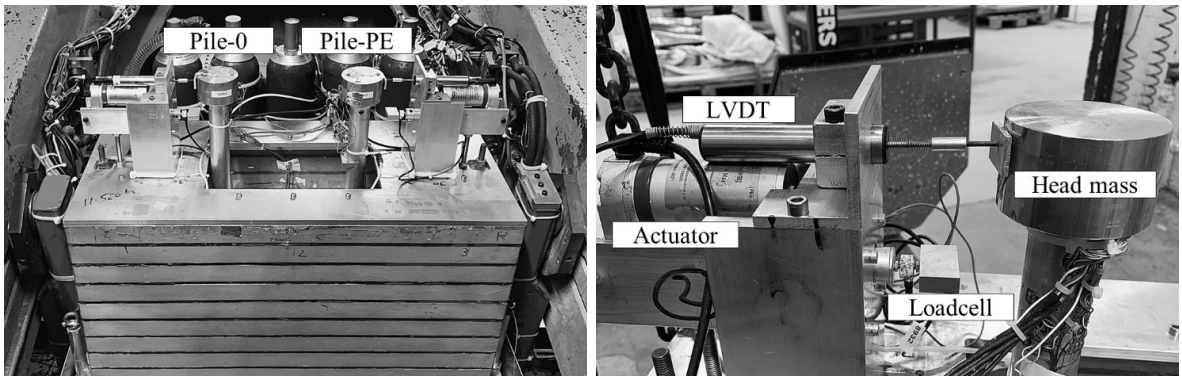

(b) (c)

Figure 2. Test model: (a) schematic representation and (b,c) photo of the test set-up

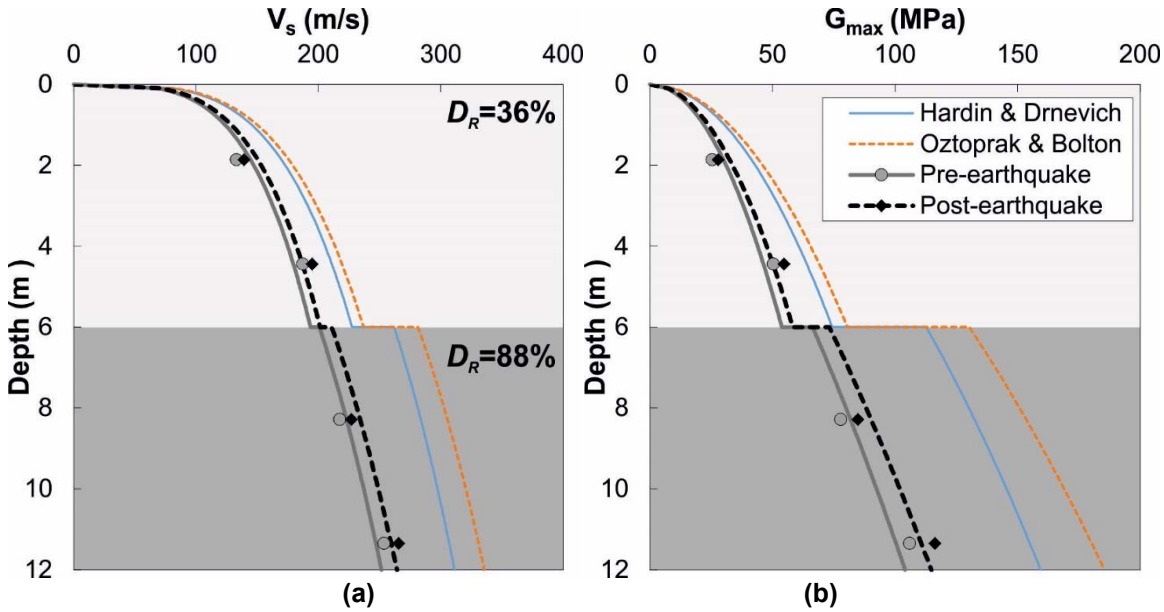

(a) (b)

Figure 3. Evolution of measured (a) shear wave velocity and (b) small strain shear modulus with depth and comparison with theoretical profiles from Hardin and Drnevich (1972) and Oztoprak and Bolton (2013)

Ground motion

A series of horizontal input motion was applied at the bedrock level using a servo-hydraulic earthquake actuator. The series of ground motions applied is detailed in Table 3. In this paper, the results from the following input motions are considered:

- Test EQ1: A sine sweep of increasing frequencies from 0~1 Hz, which enabled to establish the natural frequency of the pile-soil system.
- Test EQ5: A series of 10 cycles at the natural frequency 0.5 Hz (30 Hz model scale)
- Test EQ6:A series of 10 cycles at twice the natural frequency 1 Hz (60 Hz model scale)
- Test EQ8: A final sine sweep at increasing frequencies post - strong earthquakes.

Horizontal load

Finally, a horizontal push was applied to the pile using a displacement-controlled actuator. The pile-top displacement was checked using LVDTs, which reached their final stroke along the monotonic test at 0.38 m for Pile-PE and 0.17 m for Pile-0. Extrapolation of the data was then achieved for both piles, assuming a linear push from the actuator.

Data acquisition

The instrumentation used to monitor both pile deformation and ground motion during earthquakes consisted of miniature piezoelectric accelerometers, located as shown in Figure 2(a). Pile displacement and horizontal load during monotonic loading were recorded using a linear variable differential transducer (LVDT) and a load-cell, located at the top of the pile and at the point of load application respectively (Figure 2(c)). The accelerometers located at the top of the pile also enabled to derive the pile rotation.

SEISMIC RESPONSE

The results of the pile-head response to the input ground motions EQ1, 5, 6 and 8 are shown in Figure 4. The response to the initial sine sweep (Test EQ1, Figure 4(a)) shows that the natural frequency of the structure is 0.5 Hz at prototype scale (30 Hz model scale). The final sine sweep (Figure 4(b)) shows that the natural frequency of the structure post-earthquake is comparable to the original pre-earthquake first mode of vibration, suggesting that the dynamic stiffness of the pile-soil system is relatively unchanged.

The large earthquake of 10 cycles at 0.5 Hz prototype scale (30 Hz model scale) shows a large resonance effect of the structure in first mode, even for a small magnitude of the earthquake (Figure 4(c), Table 3), with an amplification factor of 5.2. When a higher frequency earthquake at 1 Hz prototype scale (60 Hz model scale) is applied (Figure 4(d)), the pile top response is much smaller compared to 0.5 Hz earthquakes with a reduced amplification factor of 0.8. Figure 4(d) also reveals a strong amplification at 0.5 Hz, although the amplification has very little energy present at this frequency. This is due to the resonance effects as before.

Table 3. Characteristics of ground motions (*sat : MEMS saturated, cannot obtain peak)

EQ No.		**EQ1**	EQ2	EQ3	EQ4	**EQ5**	**EQ6**	EQ7	**EQ8**
Peak acceleration (g)	Input	**0.05**	0.13	0.13	0.1	**0.05**	**0.15**	0.12	**0.05**
	Top pile	**0.2**	0.09	*sat	*sat	**0.26**	**0.12**	0.06	**0.31**
No of cycles		**Sweep**	Kobe	15	15	**15**	**15**	15	**Sweep**
Frequency (Hz)		**0-1**		0.5	0.5	**0.5**	**1**	1.5	**0-1**
Duration (prototype, s.)		**80**	10	30	30	**30**	**15**	10	**80**
Amplification factor (top pile/input)		**4**	-	-	-	**5.2**	**0.8**	-	**6.2**

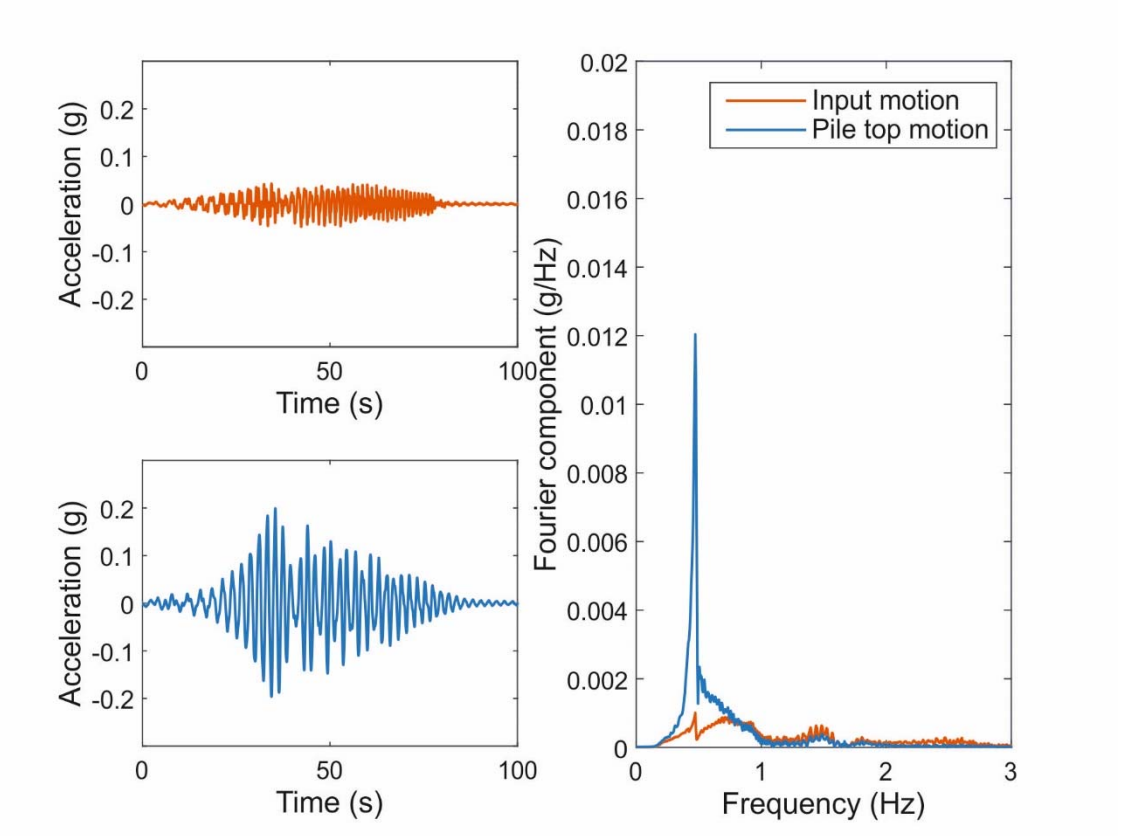

(a) Test EQ1 – Sine Sweep pre-earthquake

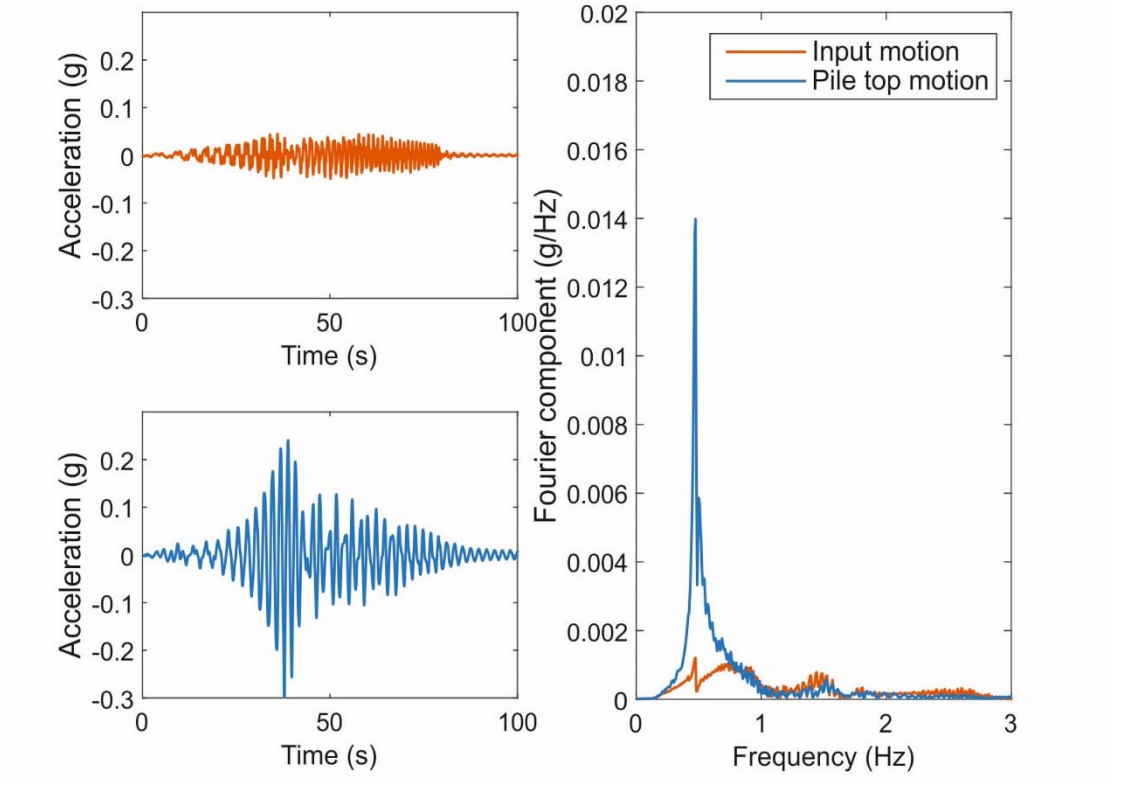

(b) Test EQ8 – Sine sweep post-earthquake

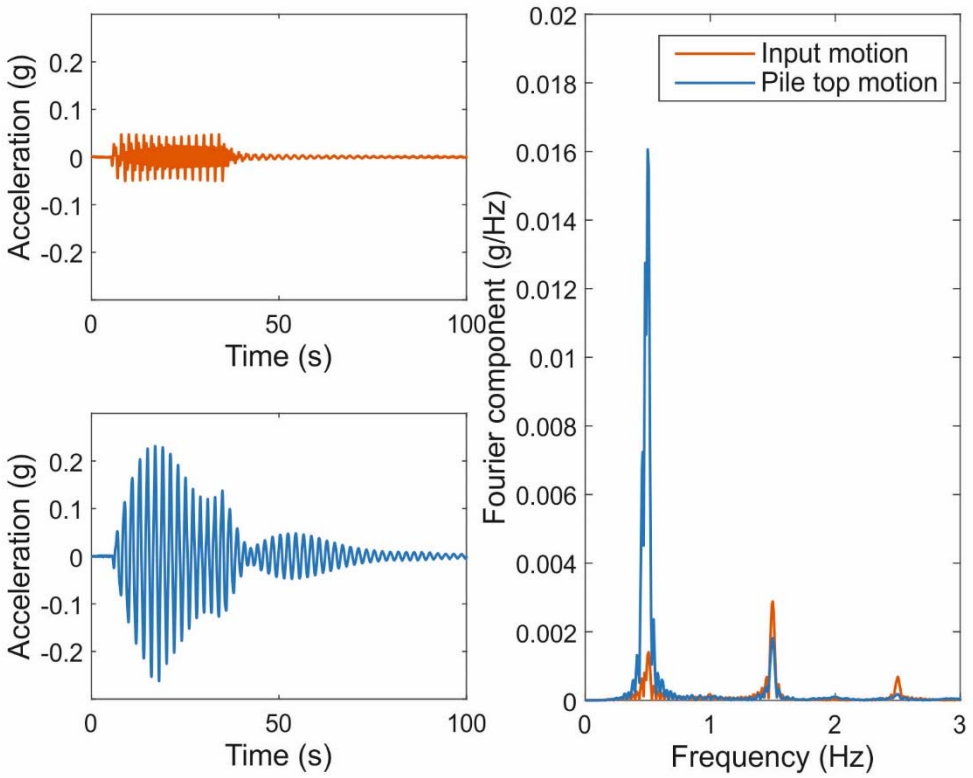

(c) Test EQ5 – Cyclic at 0.5 Hz prototype scale (30 Hz model scale)

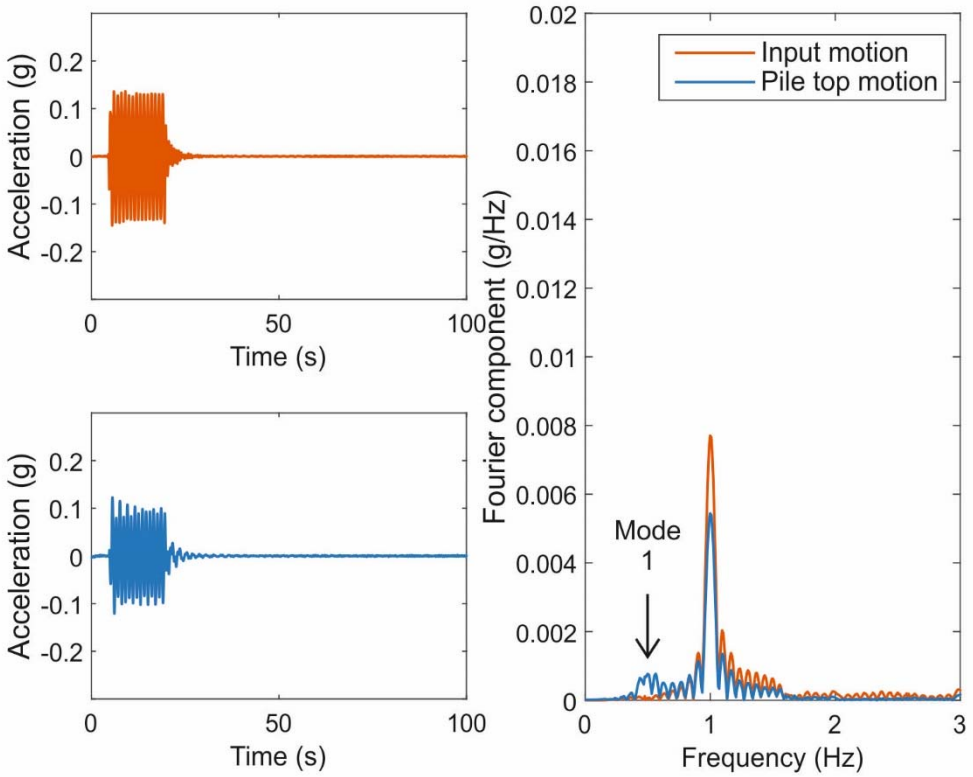

(d) Test EQ6 – Cyclic at 1 Hz prototype scale (60 Hz model scale)

Figure 4. Pile top response to EQ1,5,6 and 8 ground motions

While the amplification at resonant frequency of the pile-soil system is expected, the magnitude of this amplification is striking. In contrast the second mode of vibration (2 fn) is attenuated suggesting that the dynamic effects for second mode and higher are negligible and that the monopile is more vulnerable to earthquakes with strong, low frequency components.

POST-EARTHQUAKE MONOTONIC RESPONSE

Comparison between the pile monotonic response before (solid grey line) and post-earthquake (dashed black line) is shown in Figure 5(a,b). The horizontal load vs. pile displacement at point of load application for large displacements ($v_T = 25\%\ D$) is shown in Figure 5(a), and for small displacements ($v_T = 1\%\ D$) in Figure 5(b). The results clearly show that the pile behaviour, both in terms of stiffness and strength is affected by the earthquake history. The post-earthquake large displacement response in Figure 5(a) can be divided into three almost-elastic regions, with the initial stiffness clearly softer than the pre-earthquake pile

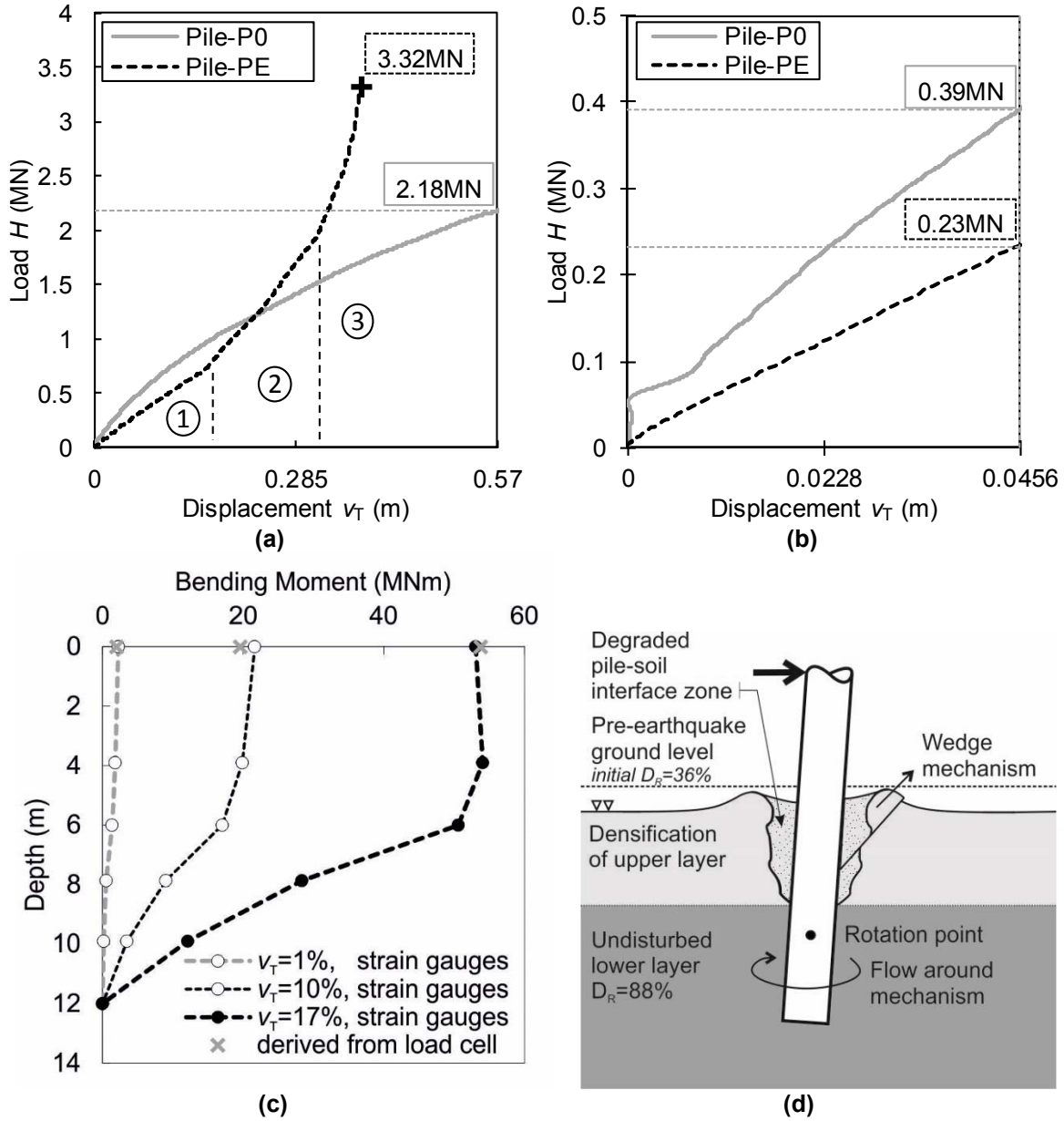

Figure 5. Pile response to monotonic loading before and after earthquakes: Load-displacement curves at (a) large ($v_T = 25\%D$) and (b) small displacements ($v_T = 1\%D$); (c) bending moment; (d) schematic representation of soil layout response post-earthquake under lateral load

stiffness (see also Figure 5(b)) and the two subsequent phases displaying increasingly large strain-hardening. This change in behaviour is hypothesized to have been caused by (i) densification of the top loose layer during the series of earthquakes, while (ii) degradation of the soil-pile interface caused by soil grains re-arrangements as the pile vibrates under each earthquake loading (Figure 5(d)). It is likely that the bottom layer relative density is not greatly affected by the earthquakes, although small changes in small strain shear modulus are observed (see Figure 3). Since the behaviour of short piles is dominated by the wedge mechanism at the top of the pile, rather than the soil flow-around at depth, when the pile is then pushed laterally, the behaviour is largely affected by the top layer grains re-arrangement: on initial loading, the behaviour is dominated by the degraded soil-pile interface, and is hence softer. Once the lateral displacements are large enough and this zone has been sufficiently loaded, the denser layer provides a stiffer lateral reaction. It is likely that there is a transition zone between the degraded zone and far-field dense zone, explaining the second portion of the dashed curve in Figure 5(b).

Finally, Figure 5(c) provides the bending moment profile of the post-earthquake pile during the final lateral load. At the soil surface, the pile bending moment could also be derived from the load-cell data multiplied by the load eccentricity, and shows good agreement with the measurements from the strain gauges close to the soil surface.

CONCLUSIONS

Pile response to earthquake loads is currently modelled by degrading the monotonic and/or cyclic response post-installation. In this paper, the pile response during and post-earthquake was evidenced via a dynamic centrifuge experiment. Two identical piles were installed in a dense layer of sand, overlaid by a loose layer of the same sand. The first pile was laterally loaded prior to triggering any ground motions, to establish the initial pile capacity, while the second pile, instrumented with strain gauges, was used to record the earthquake response and estimate the subsequent monotonic pile response.

It was concluded that the pile response to ground motions close to the first mode of resonance displays large amplification that require further investigation for development of design guidelines. Furthermore, the pile response to post-earthquake lateral loading is greatly affected by the re-arrangement of the loose layer grains over the earthquake history. The monotonic behaviour differs from the pre-seismic monotonic behaviour and is unlikely to be captured via degradation of the monotonic *p-y* curves.

ACKNOWLEDGEMENTS

The authors are thankful to the assistance of the technicians from the Schofield Centre, who helped carrying out the test, as well as the help of Jad Boksmati, Alessandro Fusco and Thejesh Kumar Garala who advised on test set-up and calibration.

REFERENCES

Abadie, C.N., 2015. Cyclic Lateral Loading of Monopile Foundations in Cohesionless Soils (DPhil). University of Oxford.

Abadie, C.N., Burd, H.J., Byrne, B.W., Houlsby, G.T., McAdam, R.A., 2020. Example modelling of monopile lifetime performance for offshore wind applications, in: 4th International Symposium on Frontiers in Offshore Geotechnics. Austin, Texas.

Achmus, M., Kuo, Y.-S., Abdel-Rahman, K., 2009. Behavior of monopile foundations under cyclic lateral load. Computers and Geotechnics 36, 725–735. https://doi.org/10.1016/j.compgeo.2008.12.003

Andersen, K., 2015. Cyclic soil parameters for offshore foundation design. The 3rd McClelland Lecture.

Brennan, A.J., Madabhushi, S.P.G., Houghton, N.E., 2006. Comparing laminar and equivalent shear beam (ESB) containers for dynamic centrifuge modelling. Presented at the Physical Modelling in Geotechnics, 6th ICPMG'06 - Proceedings of the 6th International Conference on Physical Modelling in Geotechnics, pp. 171–176.

Byrne, B.W., Burd, H.J., Zdravkovic, L., Abadie, C.N., Houlsby, G.T., Jardine, R.J., Martin, C.M., McAdam, R.A., Pacheco Andrade, M., Pedro, A.M.G., Potts, D.M., Taborda, D.M.G., 2019. PISA Design Methods for Offshore Wind Turbine Monopiles, in: Offshore Technology Conference. Presented at the Offshore Technology Conference, Offshore Technology Conference, Houston, Texas. https://doi.org/10.4043/29373-MS

Chian, S.C., Stringer, M.E., Madabhushi, S.P.G., 2010. Use of automatic sand pourers for loose sand models, in: Proceedings of the 7th International Conference on Physical Modelling in Geotechnics. Presented at the Physical Modelling in Geotechnics, Zurich, Switzerland, pp. 117–121.

Cox, W.R., Reese, L.C., Grubbs, B.R., 1974. Field Testing of Laterally Loaded Piles in Sand, in: Proceedings of the Sixth Annual Offshore Technology Conference, Houston, Texas.

DNV, 2014. Offshore Standard DNV-OS-J101, Design of offshore wind turbine structures (last edition).

DNV-GL, 2019. Alleviating Cyclone and Earthquake Challenges for Wind farms (ACE) [WWW Document]. New Joint Industry Project kicks-off to reduce cyclone and earthquake challenges for wind turbines. URL https://www.dnvgl.com/news/new-joint-industry-project-kicks-off-to-reduce-cyclone-and-earthquake-challenges-for-wind-turbines-164399

Hardin, B., Drnevich, V., 1972. Shear Modulus and Damping in Soils: Design Equations and Curves. J. Soil Mech. Found. Div. 98.

Jeanjean, P., Zhang, Y., Zakeri, A., Andersen, K., Gilbert, R., Senanayake, A., 2017. A Framework for Monotonic P-Y Curves in Clays, in: Offshore Site Investigation Geotechnics 8th International Conference Proceedings. https://doi.org/10.3723/osig17.108

Kim, D.H., Lee, S.G., Lee, I.K., 2014. Seismic fragility analysis of 5 MW offshore wind turbine. Renewable Energy 65, 250–256. https://doi.org/10.1016/j.renene.2013.09.023

Kirkwood, P.B., 2015. Cyclic lateral loading of monopile foundations in sand (PhD Thesis). University of Cambridge.

Klinkvort, R.T., 2012. Centrifuge modelling of drained lateral pile-soil response (PhD Thesis). DTU.

Lau, B., 2015. Cyclic behaviour of monopile foundations for offshore wind turbines in clay (PhD Thesis). University of Cambridge.

LeBlanc, C., Byrne, B.W., Houlsby, G.T., 2010a. Response of stiff piles to random two-way lateral loading. Géotechnique 60, 715–721. https://doi.org/10.1680/geot.09.T.011

LeBlanc, C., Houlsby, G.T., Byrne, B.W., 2010b. Response of stiff piles in sand to long-term cyclic lateral loading. Géotechnique 60, 79–90. https://doi.org/10.1680/geot.7.00196

Madabhushi, G., 2014. Centrifuge Modelling for Civil Engineers. CRC Press.

Oztoprak, S., Bolton, M.D., 2013. Stiffness of sands through a laboratory test database. Géotechnique 63, 54–70. https://doi.org/10.1680/geot.10.P.078

Peralta, P., 2010. Investigations on the Behavior of Large Diameter Piles under Long-Term Lateral Cyclic Loading in Cohesionless Soil (PhD Thesis). University of Hannover.

Puech, A., 2017. Recommandations pour le dimensionnement des pieux sous chargements cycliques projet national SOLCYP.

Reese, L.C., Cox, W.R., Koop, F.D., 1974. Analysis of laterrally loaded piles in sand, in: Proceedings of the 6th Offshore Technology Conference, Houston 2.

Schofield, A.N., 1980. Cambridge Geotechnical Centrifuge Operations. Géotechnique 30, 227–268. https://doi.org/10.1680/geot.1980.30.3.227

Zhang, Y., Andersen, K., Klinkvort, R.T., Jostad, H., Sivasithamparam, N., Boylan, N., Langford, T., 2016. Monotonic and Cyclic p-y Curves for Clay Based on Soil Performance Observed in Laboratory Element Tests. https://doi.org/10.4043/26942-MS